MERATECH
Vol. 01, No. 1 (2025), pp. 28-37
ISSN: XXXX-XXXX

IoT-Based Real-Time Wind Power Plant Monitoring and Overload Protection

Ahmad Farobi Abdurrohim[1] | Langlang Gumilar[2*] | Slamet Wibawanto[3]

[1]Study Program of Power Plant Engineering Technology, Faculty of Vocational, Universitas Negeri Malang, Malang 65145, Indonesia | [2]Department of Electrical Engineering and Informatics, Faculty of Engineering, Universitas Negeri Malang, Malang 65145, Indonesia

Corresponding Author: Langlang Gumilar (langlang.gumilar.ft@um.ac.id)

Received: 28-08-2025 | **Accepted:** 31-08-2025

Abstract
Wind Power Plants (WPP) are an environmentally friendly renewable energy solution. However, ensuring optimal performance and operational safety requires a reliable monitoring and protection system. This research focuses on the development and implementation of an Internet of Things (IoT)-based monitoring system for real-time tracking of current, voltage, power, RPM, and wind speed parameters, along with an automated overload protection mechanism. The system is designed to be accessible and controllable via a web platform. The methodology involves hardware and software design, integrating a microcontroller with the Thinger.io platform, which also facilitates remote relay control for WPP and inverter outputs. The protection system is configured to detect overload conditions and trigger automatic disconnection while delivering real-time notifications through Telegram. Experimental results indicate that the overload protection mechanism operates with high reliability, achieving an average response time of 0.96 seconds. The IoT integration via Thinger.io proved effective in enabling data visualization, remote device control, and responsive real-time notifications. Sensor accuracy was maintained with measurement errors below 10% for most primary parameters. Additionally, the system demonstrated optimal efficiency at a wind speed of 7 m/s, with a linear correlation observed between wind speed and electrical output. This research confirms that IoT-based monitoring and protection systems enhance the safety and ease of operational supervision for WPPs in a sustainable manner.

Keywords: Wind Power Plant, Internet of Things, Overload Protection, PZEM017, PZEM004T, Anemometer Sensor, IR Sensor

1. INTRODUCTION

Wind Power Plants (WPP) constitute a sustainable renewable energy solution that utilizes wind energy to generate electrical power. One of the main environmental advantages of WPP is its ability to operate without emitting greenhouse gases, making it a clean alternative to conventional fossil-fuel-based power generation [1]. With the rapid advancement of renewable energy technologies, wind power is projected to play a central role in fulfilling the growing global demand for sustainable and clean electricity in the near future [2]. However, the effective operation of WPP requires not only optimal design and installation but also continuous and precise monitoring to ensure that performance remains within safe and efficient operational parameters [3]. Without proper monitoring, even minor deviations in operating conditions can lead to system inefficiencies, reduced lifespan of components, or unexpected failures that impact the overall reliability of power generation systems [4]. Therefore, the implementation of robust and advanced monitoring solutions in WPP is an essential component in maintaining both operational stability and environmental sustainability.

Real-time monitoring systems in WPP provide critical insight into operational variables such as electrical current, voltage, and turbine rotational speed [5]. By consistently tracking these parameters, operators can detect anomalies or early signs of malfunction, thereby enabling preventive measures before these issues escalate into costly downtime or irreversible damage [6]. Additionally, collected monitoring data can serve as a valuable resource for performance evaluation, operational optimization, and strategic maintenance planning [7]. This information supports data-driven decision-making processes, which are increasingly important in modern energy management [8]. The introduction of Internet of Things (IoT) technology into wind energy monitoring has further enhanced this capability, offering the possibility of real-time, remote data access and control [9]. IoT-based monitoring not only improves efficiency but also increases operational safety by allowing immediate intervention when abnormal conditions are detected, making it a priority area of development for modern WPP operations [10].

In addition to monitoring capabilities, protection systems form a critical layer of safety in wind power plant operations [11]. These systems are specifically designed to detect abnormal electrical conditions such as overcurrent, overvoltage, or short circuits and initiate rapid disconnection of the affected circuits to prevent equipment damage or hazards to personnel [12]. Common protection mechanisms include relays, circuit breakers, and fuses, which act as automated safety barriers against potentially damaging events [13]. Effective protection systems contribute to both the reliability and efficiency of electrical power delivery by preventing unnecessary system interruptions and avoiding physical damage to components [14]. In renewable energy systems like WPP, where the operating environment is highly dynamic, protection systems are particularly

important due to fluctuating wind conditions and variable electrical loads. Therefore, the integration of advanced protection mechanisms directly into the monitoring framework provides a holistic approach to operational safety and system longevity.

The concept of the Internet of Things plays an increasingly important role in the advancement of renewable energy systems. IoT involves the interconnection of hardware and software devices over the internet, enabling automated data collection, analysis, and communication between devices without the need for human intervention [15]. In the context of WPP, IoT technology facilitates the remote monitoring of operational parameters such as voltage, current, power output, turbine rotational speed, and wind velocity. These data can be transmitted to cloud-based platforms like Thinger.io, allowing operators to visualize real-time system performance, receive early warnings for abnormal conditions, and execute remote control commands when necessary [16]. Furthermore, IoT-based systems can integrate with automated notification services, such as Telegram alerts, to ensure that operators are promptly informed of any critical operational events [17]. This integration enables faster response times, reduces downtime, and improves the overall resilience of wind power systems [18].

Motivated by these operational needs, the present study proposes the design and development of an IoT-based monitoring and overload protection system for WPP. The proposed system integrates multiple sensors with an ESP32 microcontroller and the Thinger.io platform to enable real-time tracking of electrical and mechanical parameters, automated protective responses, and cloud-based control functionalities. By combining continuous monitoring with automated fault protection, the system is expected to enhance the efficiency, safety, and sustainability of WPP operations. This research aims not only to demonstrate the technical feasibility of such a system but also to highlight its potential role in supporting the broader adoption of renewable energy solutions. Ultimately, the findings of this study contribute to the optimization of operational performance in WPP, supporting long-term goals of energy security, environmental preservation, and technological innovation in the renewable energy sector.

2. METHOD

2.1. Hardware Development

This section elaborates on the hardware design process, focusing on the selection and specification of components necessary for an efficient IoT-based monitoring system for Wind Power Plants (WPP). The hardware configuration is illustrated in Figure 1, depicting the integration of sensors, microcontroller units, and communication modules.

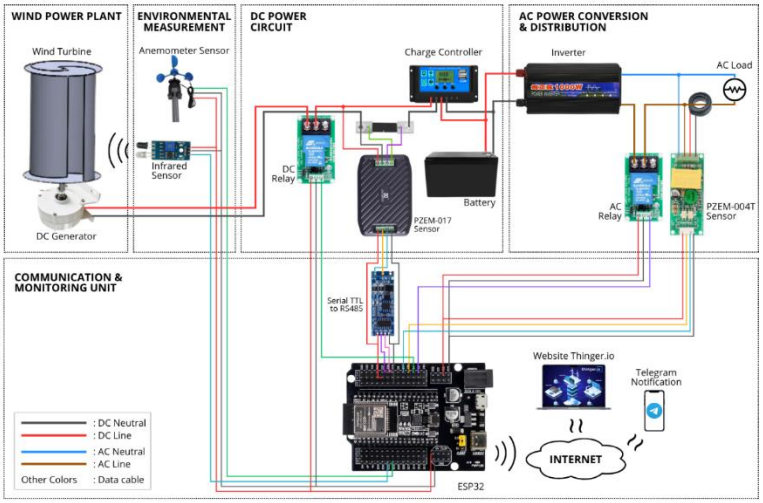

Figure 1. Hardware System Schematic

As shown in Figure 1, the proposed hardware architecture facilitates real-time monitoring of WPP parameters through the Thinger.io platform. The ESP32 microcontroller serves as the core controller, aggregating data from multiple sensors. Electrical parameters from the generator output are monitored using the PZEM-017 module, while the PZEM-004T sensor captures data from the AC output, including current, voltage, and power measurements. An IR sensor is employed to determine the rotational speed (RPM) of the wind turbine, whereas an anemometer module measures wind velocity.

The ESP32 is tasked with processing and transmitting the acquired data to Thinger.io, where it is visualized through a web interface. The monitored parameters include electrical current, voltage, power, RPM, wind speed, and system status, indicating normal operation or fault conditions such as short circuits. The electrical output power is computed based on current and voltage readings using the equation [19]:

$$P_g = V \times I \quad (1)$$

where P_g denotes the generator output power in Watts, V is the voltage in Volts, and I is the current in Amperes.

Relay module acts as a protective switch, disconnecting the load from both AC and DC circuits in the event of abnormal conditions. Upon detecting a short circuit, the system will display an "OVERLOAD" status on the website and issue a Telegram

notification with the message "AC/DC OVERLOAD DETECTED". To ensure operational safety, the control functions on the website are enabled only when system parameters fall below predefined thresholds: voltage below 14VDC or 250VAC, current is under .15A DC or 1.5A AC, and power consumption does not exceed 1.5W DC or 25W AC, ensuring that system reconnections are performed under safe conditions.

2.2. Software Design

The software design phase focuses on integrating sensor data acquisition with cloud-based monitoring and control via Thinger.io. The software is developed using the Arduino IDE, ensuring adherence to best coding practices and thorough unit testing for reliable system performance.

The program logic encompasses data acquisition, processing, and transmission routines for all integrated sensors, enabling real-time visualization of WPP operational data on the Thinger.io platform. The overall software architecture is represented in Figure 2.

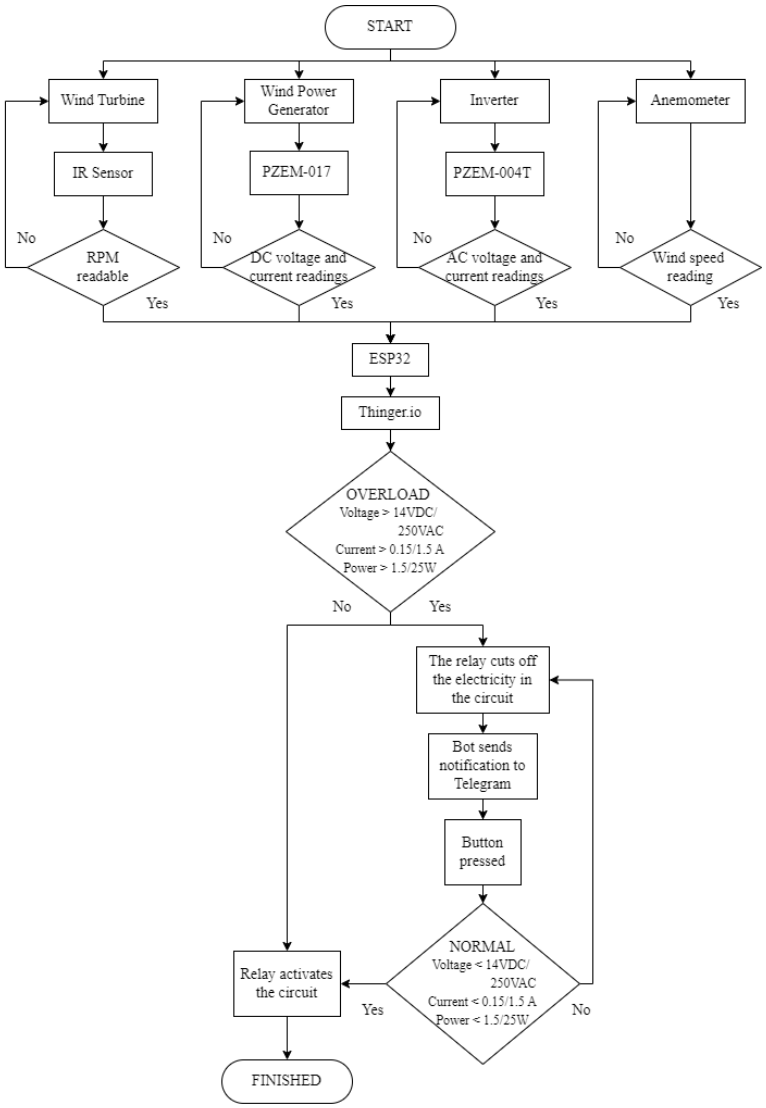

Figure 2. Software System Schematic

Figure 2 presents the software system architecture, in which the ESP32 microcontroller functions as the primary data acquisition unit, aggregating measurements from multiple sensors. The PZEM-017 module is responsible for capturing DC output parameters from the generator, whereas the PZEM-004T module monitors AC output, including current, voltage, and power levels. Turbine rotational velocity is obtained via an infrared (IR) sensor, while an anemometer module measures the ambient wind speed.

Upon acquisition, all sensor data including current, voltage, power, RPM, and wind velocity are processed locally by the ESP32 before being transmitted to the Thinger.io cloud platform. This integration allows for remote monitoring and control, providing a user interface that displays operational parameters in real time, such as electrical measurements and the system's operational state (normal or short-circuit).

The software also incorporates a protection control feature through relay actuation. The relay disconnects DC or AC loads in response to abnormal conditions. In short-circuit scenarios, the web platform automatically issues an "OVERLOAD" status

message, and a Telegram-based alert system notifies users with the message "AC/DC OVERLOAD DETECTED," enabling rapid operator response. Control buttons on the web platform are programmed with operational constraints—activation is permitted only when voltage remains below 14 VDC or 250 VAC, current is under 0.15 A DC or 1.5 an AC, and power does not exceed 1.5 W DC or 25 W AC—thereby ensuring safe system recovery following a fault event.

2.3. Data Analysis

Data analysis is conducted to assess the system's performance in terms of monitoring accuracy and operational efficiency. The collected data serves as a foundation for system validation, identifying areas for improvement and informing future system enhancements.

Sensor validation involves calculating absolute and relative errors to determine the accuracy and reliability of sensor readings across various scenarios [20]. Absolute error represents the absolute difference between the measured sensor value and the reference standard, formulated as [21]:

$$E_a = |xi\text{-}xp| \quad (2)$$

where xi is the value obtained from the sensor and xp is the corresponding reference measurement.

This metric reflects the magnitude of deviation without considering its direction. Relative error, on the other hand, provides a normalized measure of error by expressing it as a percentage of the reference value, as given by [21]:

$$E_r = \frac{Ea}{xp} \times 100\% = \frac{|xi\text{-}xp|}{xp} \times 100\% \quad (3)$$

Relative error facilitates comparative analysis across different measurement ranges, offering a comprehensive view of sensor performance. According to IEC Standard 13B-23, sensors are deemed accurate and reliable if their measurement errors remain within ±5% of the reference values provided by calibrated measuring instruments such as multimeters, tachometers, and anemometers [22].

3. RESULTS AND DISCUSSION

3.1. Experimental Results and Performance Evaluation

Comprehensive testing was conducted to assess the system's functionality across key parameters: wind speed, turbine rotational speed (RPM), DC generator power output, inverter power output under AC load, relay-based overcurrent protection in DC and AC circuits, and the system's real-time data visualization via Thinger.io. Each parameter was evaluated using integrated sensors interfaced with an ESP32 microcontroller to determine system effectiveness across various operational scenarios.

3.1.1. Anemometer Performance Testing

Table 1. Wind Speed Measurement Results (m/s)

Wind Speed (m/s)	Anemometer Module (m/s)	Error (%)
4	4.65	16.25%
4.5	4.9	8.89%
5	5.31	6.20%
5.5	5.78	5.09%
6	6.13	2.17%
6.5	6.44	0.92%
7	7.07	1.00%
7.5	7.6	1.33%
8	8.04	0.50%
Average Error		**4.71%**

Results from Table 1 indicate that the sensor consistently detected wind speed increments, with recorded values between 4.65 m/s and 8.04 m/s. The maximum error of 16.25% occurred at the lowest tested wind speed (4 m/s), highlighting a slight underestimation tendency at low speeds. However, accuracy improved substantially for speeds above 5 m/s, with errors dropping below 6.2% and reaching optimal accuracy levels (<1%) within the 6.5–8 m/s range. The sensor's average error of 4.71% confirms its reliability for small-scale WPP monitoring.

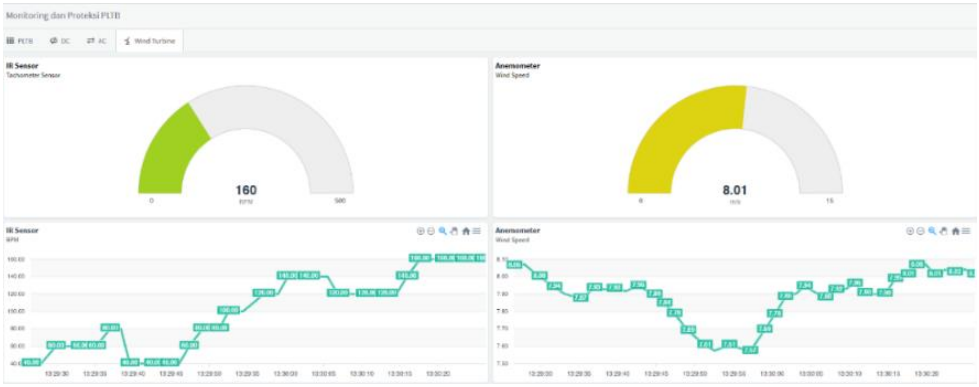

Figure 3. Wind Turbine Tab Menu View on Thinger.io

The user interface on Thinger.io, as shown in Figure 3, displays real-time readings of wind speed (m/s) from the anemometer and turbine RPM from the IR sensor, accompanied by data graphs tracking parameter changes over 10 minutes. Table 1 details the anemometer's wind speed measurements compared to a reference anemometer, computed using Equation (2) & (3), across a 4–8 m/s range in 0.5 m/s increments.

3.1.2. Infrared Sensor Accuracy Testing

Table 2 compares the RPM measurements from the IR sensor with a digital tachometer, benchmarked through Equation (3.2). Testing spanned wind speeds from 4 to 8 m/s at 0.5 m/s intervals, yielding nine data points that illustrate the correlation between wind velocity and turbine RPM.

Both methods displayed a strong positive correlation, with maximum RPMs recorded at 8 m/s (280.3 RPM via tachometer and 290 RPM via IR sensor). At 4 m/s, the tachometer recorded 76.7 RPM, while the IR sensor measured 105 RPM. Error analysis revealed the highest discrepancy of 36.90% at the lowest RPM, indicating accuracy limitations in low-speed conditions. Conversely, the sensor exhibited its best performance at 6.5 m/s, with an error of only 0.75%. The average error across all tests was 8.68%, confirming the IR sensor's adequacy for RPM measurement tasks.

Table 2. Wind Speed Measurement Results (m/s)

Wind Speed (m/s)	Sensor IR (rpm)	Tachometer (rpm)	Error (%)
4	105	76.7	36.90%
4.5	150	155.9	3.79%
5	217	195.4	11.05%
5.5	228	213.3	6.89%
6	246	234.6	4.86%
6.5	250	251.9	0.75%
7	254	275.2	7.70%
7.5	287	279.5	2.68%
8	290	280.3	3.46%
Average Error			**8.68%**

3.1.3. PZEM-017 Voltage and Current Measurement Testing

Voltage and current readings from the PZEM-017 sensor were recorded between 09:00 and 10:00 in 5-minute intervals and compared with a digital multimeter. Figure 4 depict the recorded voltage and current trends and the corresponding display on Thinger.io.

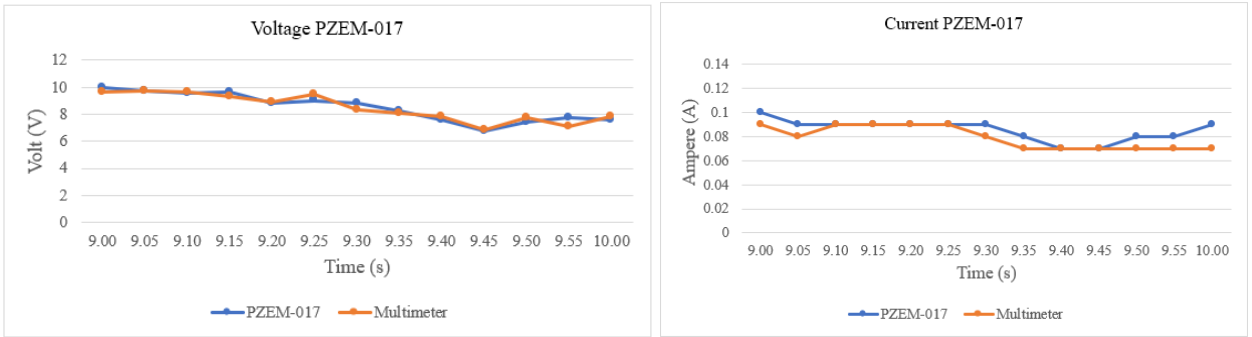

Figure 4. Test Graph of Reading Voltage and Current PZEM-017

Voltage readings ranged from 7.62 V to 9.96 V, with multimeter benchmarks slightly lower at 7.67 V to 9.75 V. The computed average voltage error was 3.33%, within acceptable error margins. Current measurements showed more variation, with PZEM-017 readings of 0.07 A to 0.10 A, while the multimeter measured 0.07 A to 0.09 A, resulting in an average current error of 8.44%. Variations in current readings were attributed to fluctuating generator outputs, particularly at low current levels.

3.1.4. PZEM-004T Inverter Output Testing

Voltage and current outputs from the PZEM-004T sensor were monitored in Figure 5, during inverter operation with a fan load, cross-referenced with multimeter measurements over a 5-minute interval from 09:00 to 10:00.

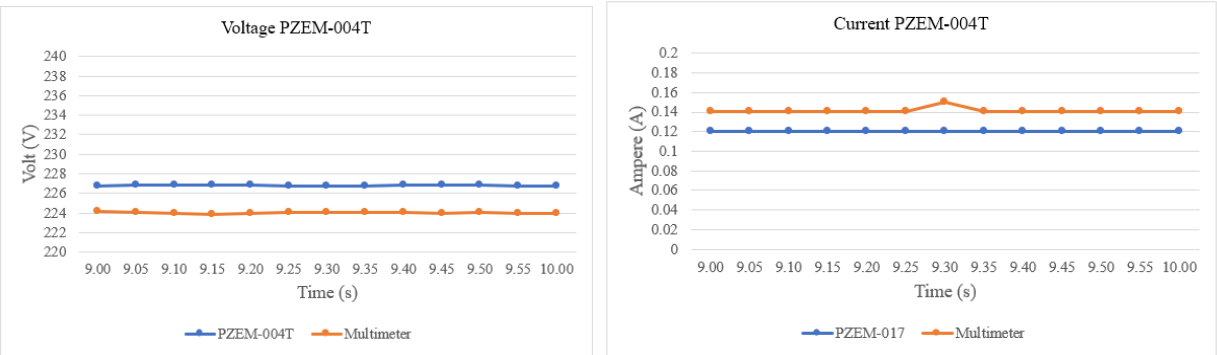

Figure 5. Test Graph of Reading Voltage and Current PZEM-004T

The sensor consistently measured voltage within 226.8–226.9 V, while the multimeter reported slightly lower readings between 223.9 V and 224.2 V. The resulting voltage error averaged 1.25%, indicating accurate and stable voltage monitoring. However, current measurements exhibited larger errors; the PZEM-004T recorded a constant 0.12 A, while the multimeter showed 0.14 A, with an outlier of 0.15 A at 09:30. The average current error stood at 14.76%, suggesting limited accuracy for low current measurements under 0.5 A.

3.1.5. Relay Control Response Evaluation

Relay control tests assessed the system's responsiveness and reliability in both normal and overload conditions via the Thinger.io interface. Table 3 summarizes the results, indicating an average response time of 0.96 seconds across 16 trials with consistent execution of ON/OFF commands and status synchronization.

Table 3. Relay Button Test Results on the Thinger.io Website

Command	Relay Status	Response Time (Second)	Details
ON	Normal (DC)	1.1	Button ON, relay active
OFF	Normal (DC)	1.6	Button OFF, relay disabled
ON	Normal (DC)	0.8	Button ON, relay active
OFF	Normal (DC)	0.9	Button OFF, relay disabled
ON	Normal (AC)	1.3	Button ON, relay active
OFF	Normal (AC)	1.1	Button OFF, relay disabled
ON	Normal (AC)	0.7	Button ON, relay active
OFF	Normal (AC)	0.9	Button OFF, relay disabled
ON	Overload (DC)	0.8	Relay is forced to OFF
ON	Overload to Normal (DC)	0.7	The button can activate the relay
ON	Overload (DC)	1	Relay dipaksa OFF
ON	Overload to Normal (DC)	0.9	The button can activate the relay
ON	Overload (AC)	1	Relay is forced to OFF
ON	Overload to Normal (AC)	0.9	The button can activate the relay
ON	Overload (AC)	0.8	Relay is forced to OFF
ON	Overload to Normal (AC)	1	The button can activate the relay

In overload scenarios, the system automatically disengaged the relay with a recovery time of 0.88 seconds. Table 4 shows that response times remained below 2 seconds, with most activations occurring within 0.7 to 1.0 seconds. Recovery times consistently remained under 1 second, demonstrating the efficiency and reliability of the microcontroller-based protection mechanism.

Table 4. Relay Control System Performance Statistics

Parameter	Average	Min	Max
Response Time (Second)	0.96	0.7	1.6
Recovery Overload Time	0.88	0.7	1.0

3.2. Performance Analysis

This section presents a comprehensive discussion of the system's performance, focusing on critical parameters such as wind speed, turbine RPM, DC and AC voltage/current, DC generator output power, inverter operation, and the Thinger.io web interface for real-time monitoring and control.

3.2.1. Analysis of Wind Speed Influence on Turbine RPM and DC Generator Output

This subsection investigates the correlation between wind speed, turbine RPM, and DC voltage as observed through the Thinger.io monitoring platform. Structured data collection was performed across a wind speed range of 5–8 m/s in 0.5 m/s intervals, utilizing anemometers, tachometers, and digital multimeters as reference instruments. While RPM and voltage readings generally scaled proportionally with wind speed increases, deviations from linearity were noted beyond 7 m/s, signaling the presence of mechanical and electrical system constraints.

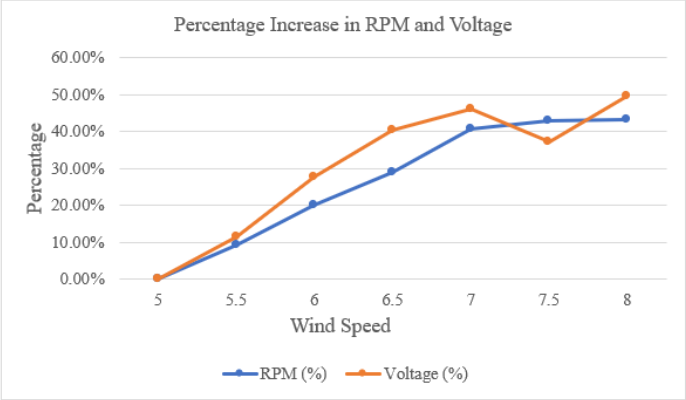

Figure 6. Percentage Increase of Parameters Relative to Baseline (5 m/s)

Figure 6 visualizes the relative cumulative increase of RPM and voltage compared to the baseline measurement at 5 m/s. RPM increased steadily, reaching a 40.8% rise at 7 m/s, but experienced significant stagnation with only a +2.6% increment as wind speed increased to 7.5–8 m/s. DC voltage exhibited its sharpest rise at 7 m/s, peaking at a 46.1% increase, followed by a decrease to 37.3% at 7.5 m/s, indicative of a voltage drop due to generator mechanical instability. Voltage increments outpaced RPM increases by approximately 2.3 times, reflecting heightened electromechanical efficiency at elevated rotational speeds. However, the anomaly at 7.5 m/s suggests limitations in generator performance, likely caused by mechanical inconsistencies.

3.2.2. DC Circuit Overload Protection Response to Load Variations

To evaluate the DC circuit's overload protection functionality, tests were conducted with varying resistive loads to determine the system's effectiveness in disconnecting power via relay based on real-time sensor feedback from the PZEM-017. The protection logic was configured to trigger when voltage exceeded 14V, current surpassed 0.15A, or power output reached 1.5W.

Table 5. DC Circuit Overload Protection Testing with 14V/ 0.15A/ 1.5W limits

Load (Ω)	Relay	Notification	Parameter	PZEM-017	Multimeter	Trip Condition
105	ON	No	Voltage (V)	9.67	9.33	Under Threshold
			Current (A)	0.10	0.095	
			Power (W)	0.8	0.88	
100	OFF	Yes	Voltage (V)	9.73	8.98	Current ≥0.15A (0.15A)
			Current (A)	0.15	0.073	
			Power (W)	1.3	0.65	
70	OFF	Yes	Voltage (V)	8.79	8.61	Current ≥0.15A (0.15A)
			Current (A)	0.15	0.12	
			Power (W)	1.3	1.4	
50	OFF	Yes	Voltage (V)	7.95	7.83	Current >0.15A (0.16A)
			Current (A)	0.16	0.16	
			Power (W)	1.2	1.25	

Table 5 provides a summary of the test results. Under a 50Ω load, the system activated protection by switching the relay OFF when the current exceeded the threshold at 0.16A, despite voltage and power remaining within safe limits. Subsequent tests with 70Ω and 100Ω loads yielded similar outcomes, with the relay disconnecting power upon reaching or exceeding the current threshold.

Conversely, at a 105Ω load, the system maintained normal operation, with all monitored parameters remaining below the protection limits. This confirms the system's ability to accurately distinguish between normal and fault conditions, ensuring reliable protective intervention.

Figure 7. Relay Status Display When Overloaded on the DC Tab Menu Website

Figure 7 displays the Thinger.io interface showing the DC relay status in the OFF state during an overload event. This real-time visualization highlights the system's capability to isolate faults effectively while providing immediate feedback to the user.

3.2.3. AC Circuit Overload Protection Under Load Variations

The overload protection mechanism for the AC circuit was examined by subjecting the system to varying load conditions involving lamps and fans. The protection parameters were set to activate at voltage levels above 250V, current exceeding 1.5A, or power outputs greater than 25W.

Table 6. AC Circuit Overload Protection Testing with 250V/ 1.5A/ 25W limits

Load (Ω)	Relay	Notification	Parameter	PZEM-004T	Multimeter	Trip Condition
5W Lamp	ON	No	Voltage (V)	227.2	224.4	Under Threshold
			Current (A)	0.06	0.03	
			Power (W)	5.2	6.7	
7W Lamp	ON	No	Voltage (V)	227.3	224.5	Under Threshold
			Current (A)	0.09	0.05	
			Power (W)	3.5	11.2	
Low Speed Fan	ON	No	Voltage (V)	226.8	224.1	Under Threshold
			Current (A)	0.12	0.149	
			Power (W)	20.6	33.3	
High Speed Fan	ON	No	Voltage (V)	225.8	223.0	Under Threshold
			Current (A)	0.15	0.179	
			Power (W)	24.0	39.9	
5W Lamp + Low Fan	ON	No	Voltage (V)	227.2	224.5	Under Threshold
			Current (A)	0.11	0.125	
			Power (W)	23.6	28.0	
Low Fan + 7W Lamp	OFF	Yes	Voltage (V)	225.5	223.1	Power >25W (25.2W)
			Current (A)	0.11	0.179	
			Power (W)	25.2	39.9	
5W Lamp + High Fan	OFF	Yes	Voltage (V)	227.2	224.3	Power >25W (34.5W)
			Current (A)	0.14	0.154	
			Power (W)	27.3	34.5	

Table 6 outlines the results. Under standard operating loads (e.g., a single lamp or fan at low speed), the system remained stable without triggering protection. However, when load combinations exceeded the defined limits, the system reliably responded by disconnecting the relay and sending notifications via Thinger.io.

For instance, a combined load of a 5W lamp and a low-speed fan resulted in a power output of 25.2W, prompting a relay trip. Similarly, a combination of a 5W lamp and a high-speed fan produced 27.3W, triggering the protection mechanism. These results validate the system’s capability to detect and respond accurately to overload scenarios.

Figure 8 illustrates the AC relay status switching to OFF during an overload event, confirming that the IoT-based monitoring and protection system functions reliably in both detection and response phases.

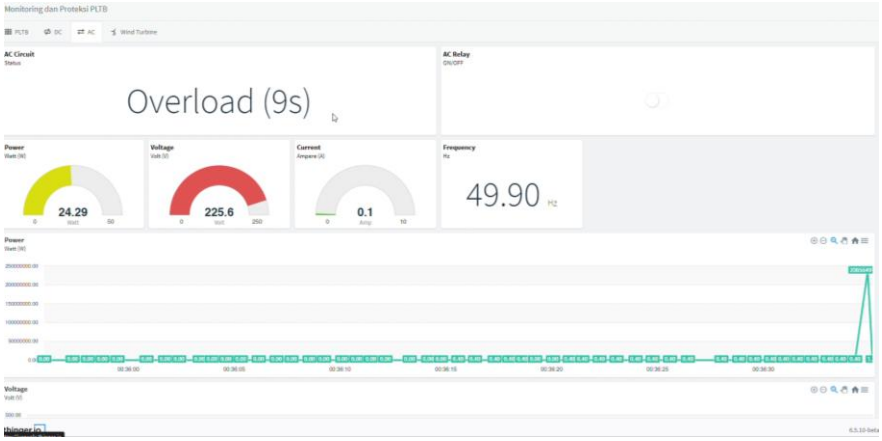

Figure 8. Relay Status Display When Overloaded on the AC Tab Menu Website

4. CONCLUSION

This study has successfully demonstrated the design and implementation of an IoT-based monitoring and protection system for Wind Power Plants (WPP), as validated through systematic testing and performance evaluations. The developed system can provide real-time monitoring of essential parameters, such as electrical current, voltage, power output, turbine rotational speed (RPM), and wind speed, via the Thinger.io platform. Additionally, the system integrates responsive relay control functionalities, allowing users to manage operational states remotely with high precision and reliability. The overload protection mechanism proved to be effective in identifying and responding to abnormal conditions, such as overcurrent, overvoltage, and overpower, by automatically disconnecting the load through relay activation. Protection thresholds were set at 14V, 0.15A, or 1.5W for DC circuits, and 250V, 1.5A, or 25W for AC circuits. Furthermore, the integration of real-time notification capabilities through Telegram enhances the system's fault response performance, enabling prompt user awareness and facilitating proactive maintenance actions. These findings confirm that the proposed system is a viable solution for enhancing the operational safety and reliability of small-scale WPP monitoring applications.

REFRENCES

[1] S. Aroonsrimorakot, M. Laiphrakpam, and W. Paisantanakij, “Application of Innovative Eco-Friendly Energy Technology for Sustainable Agricultural Farming,” in Green Technological Innovation for Sustainable Smart Societies, C. Chakraborty, Ed., Cham: Springer International Publishing, 2021, pp. 211–231. doi: 10.1007/978-3-030-73295-0_10.

[2] M. Swadi, D. J. Kadhim, M. Salem, F. M. Tuaimah, A. S. Majeed, and A. J. Alrubaie, “Investigating and predicting the role of photovoltaic, wind, and hydrogen energies in sustainable global energy evolution,” Glob. Energy Interconnect., vol. 7, no. 4, pp. 429–445, 2024.

[3] L. Kou et al., “Review on monitoring, operation and maintenance of smart offshore wind farms,” Sensors, vol. 22, no. 8, p. 2822, 2022.

[4] İ. Alagöz, M. Bulut, V. Geylani, and A. Yıldırım, “Importance of real-time hydro power plant condition monitoring systems and contribution to electricity production,” Turk. J. Electr. Power Energy Syst., vol. 1, no. 1, pp. 1–11, 2021.

[5] H. Badihi, Y. Zhang, B. Jiang, P. Pillay, and S. Rakheja, “A comprehensive review on signal-based and model-based condition monitoring of wind turbines: Fault diagnosis and lifetime prognosis,” Proc. IEEE, vol. 110, no. 6, pp. 754–806, 2022.

[6] A. H. Adepoju, B. Austin-Gabriel, O. Hamza, and A. Collins, “Advancing monitoring and alert systems: A proactive approach to improving reliability in complex data ecosystems,” IRE J., vol. 5, no. 11, pp. 281–282, 2022.

[7] A. Bousdekis, K. Lepenioti, D. Apostolou, and G. Mentzas, “A review of data-driven decision-making methods for industry 4.0 maintenance applications,” Electronics, vol. 10, no. 7, p. 828, 2021.

[8] A. Bousdekis, K. Lepenioti, D. Apostolou, and G. Mentzas, “A review of data-driven decision-making methods for industry 4.0 maintenance applications,” Electronics, vol. 10, no. 7, p. 828, 2021.

[9] S. Karad and R. Thakur, “Efficient monitoring and control of wind energy conversion systems using Internet of things (IoT): a comprehensive review,” Environ. Dev. Sustain., vol. 23, no. 10, pp. 14197–14214, Oct. 2021, doi: 10.1007/s10668-021-01267-6.

[10] M. Mitolo, Principles and Practices of Electrical Safety Engineering: Ensuring Protection in Electrical Systems. CRC Press, 2025. Accessed: Jun. 15, 2025. [Online]. Available: https://books.google.com/books?hl=en&lr=&id=90xNEQAAQBAJ&oi=fnd&pg=PP1&dq=protective+mechanisms+are+required+to+safeguard+electrical+systems+from+abnormal+conditions+that+could+otherwise+lead+to+equipment+damage+or+safety+hazards&ots=foV_khPUAz&sig=7Si0GmkMe0nRJ9HDyo5eIyAdG6o

[11] I. Alhamrouni et al., "A Comprehensive Review on the Role of Artificial Intelligence in Power System Stability, Control, and Protection: Insights and Future Directions," Appl. Sci., vol. 14, no. 14, Art. no. 14, Jan. 2024, doi: 10.3390/app14146214.
[12] K. O. Egbuwe, M. O. Onibonoje, O. F. Ikpeze, A. O. Salau, O. E. Adediji, and W. E. Chima, "Developing an Electrical Surge Protector Maintenance System," in 2024 IEEE 5th International Conference on Electro-Computing Technologies for Humanity (NIGERCON), IEEE, 2024, pp. 1–5. Accessed: Jun. 15, 2025. [Online]. Available: https://ieeexplore.ieee.org/abstract/document/10927140/
[13] B. Perea-Mena, J. A. Valencia-Velasquez, J. M. Lopez-Lezama, J. B. Cano-Quintero, and N. Muñoz-Galeano, "Circuit breakers in low-and medium-voltage DC microgrids for protection against short-circuit electrical faults: Evolution and future challenges," Appl. Sci., vol. 12, no. 1, p. 15, 2021.
[14] N. Rane, S. Choudhary, and J. Rane, "Artificial intelligence for enhancing resilience," J. Appl. Artif. Intell., vol. 5, no. 2, pp. 1–33, 2024.
[15] A. Uzoka, E. Cadet, and P. U. Ojukwu, "The role of telecommunications in enabling Internet of Things (IoT) connectivity and applications," Compr. Res. Rev. Sci. Technol., vol. 2, no. 02, pp. 055–073, 2024.
[16] J. M. Molina, A. Bustamante, and M. A. Patricio, "Vulnerability Analysis of IoT Platforms: A Case Study on Thinger.io," in Proceedings of the 14th International Conference on the Internet of Things, Oulu Finland: ACM, Nov. 2024, pp. 267–272. doi: 10.1145/3703790.3703821.
[17] P. Sivalakshmi, T. M. Inbamalar, C. M. Hari Krishnan, S. Gowtham, K. Ganesh, and J. Akash, "Intelligent weight monitoring: a telegram alert system for multi-purpose use in saline bottle management and general weighing," in 2024 IEEE International Conference on Information Technology, Electronics and Intelligent Communication Systems (ICITEICS), IEEE, 2024, pp. 1–7. Accessed: Jun. 23, 2025. [Online]. Available: https://ieeexplore.ieee.org/abstract/document/10625412/
[18] P. I. Egbumokei, I. N. Dienagha, W. N. Digitemie, E. C. Onukwulu, and O. T. Oladipo, "Automation and worker safety: Balancing risks and benefits in oil, gas and renewable energy industries," Int. J. Multidiscip. Res. Growth Eval., vol. 5, no. 4, pp. 2582–7138, 2024.
[19] Rukmini, "The analysis of power factor improvement on inductive electrical load on Sultan Hasanuddin training ship," in AIP Conference Proceedings, AIP Publishing LLC, 2023, p. 020001. Accessed: Jun. 16, 2025. [Online]. Available: https://pubs.aip.org/aip/acp/article-abstract/2675/1/020001/2877195
[20] E. Callegari et al., "The Precision, Inter-Rater Reliability, and Accuracy of a Handheld Scanner Equipped with a Light Detection and Ranging Sensor in Measuring Parts of the Body—A Preliminary Validation Study," Sensors, vol. 24, no. 2, Art. no. 2, Jan. 2024, doi: 10.3390/s24020500.
[21] R. Malaric, Instrumentation and Measurement in Electrical Engineering. Online: Universal-Publishers, 2011. Accessed: Jun. 16, 2025. [Online]. Available: https://controlengineers.ir/wp-content/uploads/2023/03/@controlengineers-Instrumentation-and-Measurement-in-Electrical-Engineering.pdf
[22] A. Sakinah, S. Bandri, A. M. N. Putra, Z. Anthony, and Y. Warmi, "Monitoring System for Solar Panel Characteristics Using the Internet of Things (IOT)," South East Asian J. Adv. Eng. Technol., vol. 1, no. 2, Art. no. 2, Mar. 2024, doi: 10.62447/seajaet.v1i2.14.